Chin. Geogra. Sci. 2013 Vol. 23 No. 5 pp. 584–593
doi: 10.1007/s11769-013-0628-3

Springer Science Press
www.springerlink.com/content/1002-0063

Sensitivity Analysis of Thermal Equilibrium Parameters of MIKE 11 Model: A Case Study of Wuxikou Reservoir in Jiangxi Province of China

WANG Qinggai, ZHAO Xiaohong, CHEN Kaiqi, LIANG Peng, LI Shibei

(*State Environmental Protection Key Laboratory of Numerical Modeling for Environment Impact Assessment*, *Appraisal Center for Environment and Engineering*, *Ministry of Environmental Protection*, *Beijing* 100012, *China*)

Abstract: Sensitivity analysis of thermal equilibrium parameters in the reservoir module of MIKE 11 model was conducted for the Wuxikou Reservoir in Jiangxi Province of China in order to apply the module to the environmental impact assessment to accurately predict water temperature of reservoirs. Results showed that radiation parameter *A* and evaporation-first parameter were much more sensitive than other parameters. The values of the radiation parameter *A* ranged from 0.10 to 0.34. The values of evaporation-first parameter varied from 0 to 10. The sensitivity of solar absorption parameters was less than that of evaporation parameter, of which light attenuation values ranged from 0.5 to 0.7, and this parameter would not impact model results if it was more than 2. Constants in Beer's law ranged from 0.2 to 0.7. Radiation parameter *B* was not more sensitive than evaporation parameter and its reasonable range was higher than 0.48. The fitting curves showed consistent changing tendency for these parameters within the reasonable ranges. Additionally, all the thermal equilibrium parameters had much more important effects on surface water temperature than deep water temperature. Moreover, if no observed data could be obtained, the local empirical value would be used to input to the MIKE 11 model to simulate the changes in the discharged outflow-water temperature qualitatively.

Keywords: MIKE 11 model; thermal equilibrium parameters; discharged outflow-water temperature; sensitivity analysis; temperature difference

Citation: Wang Qinggai, Zhao Xiaohong, Chen Kaiqi, Liang Peng, Li Shibei, 2013. Sensitivity analysis of thermal equilibrium parameters of MIKE 11 model: A case study of Wuxikou Reservoir in Jiangxi Province of China. *Chinese Geographical Science*, 23(5): 584–593. doi: 10.1007/s11769-013-0628-3

1 Introduction

The parameter sensitivity analysis is to assess the impact of parameter change on the prediction results of the model, and then determine which parameters are the key ones of a model (Lamboni *et al*., 2011), and it can provide guidance for calibrating model parameters and effectively avoiding the blindness to adjust model parameters (Zak and Beven, 1999; Xiao *et al*., 2012). The parameter sensitivity analysis is the important research content of model parameter uncertainty analysis, and it is also very necessary for model development and evaluation (Wang *et al*., 2011a; Xiao *et al*., 2011; Bai *et al*., 2012b; Borgonovo and Tarantola, 2012). Some hydrological researchers found that the application of distributed hydrological model was limited due to lack of understanding the sensitivity of the model parameter (Beven and Binley, 1992; Zak and Beven, 1999; Wang *et al*., 2011b). Screening parameter by sensitivity analysis can not only reduce the number of calibrating model parameters and improve the running efficiency of model, but also can decrease the uncertainty of these parameters

Received date: 2012-09-26; accepted date: 2012-12-24
Foundation item: Under the auspices of Research & Development Special Fund for Public Welfare Industry of Ministry of Environmental Protection (No. 201309062, 201309003)
Corresponding author: ZHAO Xiaohong. E-mail: zhaoxh@acee.org.cn

for the model prediction (Pekárová *et al.*, 2011; Bai *et al.*, 2012a; Borgonovo and Tarantola, 2012, Zhang *et al.*, 2012).

A large number of literatures have reported that the parameter sensitivity analysis was applied to different hydrological models in the past decade. Zhang *et al.* (2008) found that the main parameters of water quality analysis simulation program (WASP) model were the maximum growth rate constant of phytoplankton at 20℃ and the ratio of carbon source to chlorophyll in water by parameter sensitivity analysis. Hapuarachchi *et al.* (2001) as well as Chen and Zhang (2006) optimized the parameters of Xinan River model by using Shuffle Complex Evolution Algorithm (SCE-UA) sensitivity analysis and genetic algorithm, respectively. However, there existed some uncertainty of these parameters due to the interaction between them. Beven and Freer (2001) developed a General Livelihood Uncertainty Estimation (GLUE) method to estimate the parameter uncertainty of hydrological models. Huang and Xie (2007) analyzed the uncertainty and sensitivity of TOPMODEL parameters by using GLUE method and got a satisfactory result. However, few studies were focused on parameter sensitivity of MIKE 11 model, which would retard the applications of this model.

Reservoir module of MIKE 11 can be used to predict water temperature by vertical two-dimensional simulation, including hydrodynamic parameters and thermal equilibrium parameters *etc*. Thermal equilibrium parameters are important drivers influencing the water temperature (Jiang *et al.*, 2000; Wang *et al.*, 2009; Bai *et al.*, 2011; Pekárová *et al.*, 2011). However, little information was paid to the sensitivity analysis of these parameters impacting the water temperature of reservoirs (Fan *et al.*, 2009; Zhang and Peng, 2009). In this study, we selected Wuxikou Reservoir as a case to calculate and analyze the sensitivity of thermal equilibrium parameters in the reservoir module of MIKE 11 model. We set various values to each thermal equilibrium parameter, and analyzed the effects of these parameters on model results in order to identify the key parameters influencing water temperatures of reservoirs. We only considered the sensitivity of individual-parameter change on model results in this study, because the interactions among parameters were complex.

2 Methodology

2.1 Study area

The Wuxikou Reservoir is located in the middle reach of the Changhe River in Jiangxi Province of China (Fig. 1). It is mainly used for flood control, water supply, and power generation. It has a maximum dam-height of 41.0 m and a normal water level of 56 m. The maximum water depth in front of the dam is 35.5 m. The backwater length of the reservoir is 22.8 km. The reservoir area is 24.7 km^2 with a total reservoir storage capacity of 4.274 × 10^8 m^3 and the normal capacity of 1.73 × 10^8 m^3. The installed capacity of hydropower station is 30.0 MW. After the construction of this reservoir, the total area of open water is greatly increased. Meanwhile, the water level in front of the dam is elevated by about

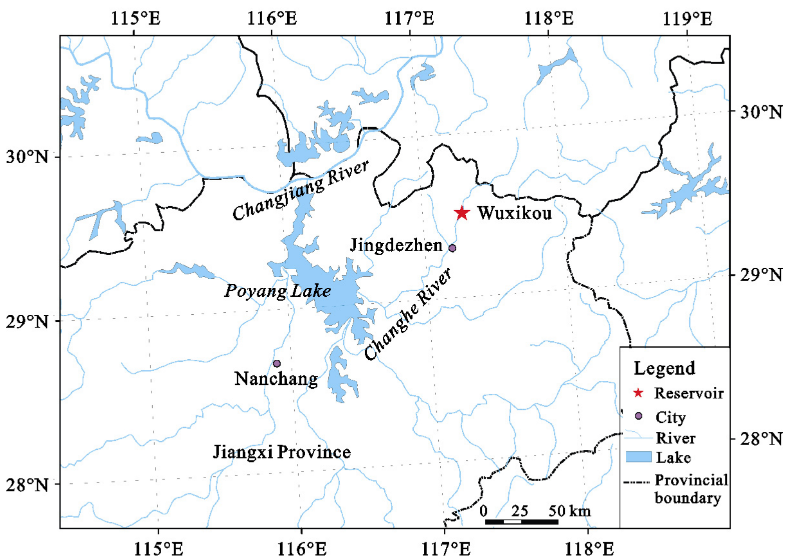

Fig. 1 Location map of Wuxikou Reservoir

20–30 m, and the average water depth is increased by about 5–8 m in the reservoir. The Wuxikou Reservoir is a seasonal storage reservoir, which does not change the inter- annual variation in runoff. The general trend of the annual variation in runoff shows a decrease in the discharge flow in wet seasons (from April to June) and an increase in the discharge flow in dry seasons (from November to the next March).

2.2 Model parameters

2.2.1 Model boundary conditions

The average flow data from the dam site of the Wuxikou Reservoir at different frequencies could be obtained from the P-III frequency curve. The average discharge at P = 75% was selected as the value in dry years. Thus we could identify that the typical dry year of this reservoir is 2004. In this study, the dry year condition would be used to predict the discharged outflow-water temperature and water temperature in front of the dam according to different values of these parameters. Base on the differences between model results, the sensitivity of these parameters was analyzed.

2.2.2 Meteorological conditions

Meteorological factors influencing the reservoir water temperature include solar radiation, air temperature, wind speed, cloud cover, and humidity. The original meteorological data input to MIKE 11 model for numerical modeling include air temperature, relative humidity, and sunshine hours. Because both solar radiation and cloud cover can be calculated by sunshine hours and wind speed data is difficult to obtain, we collected monthly average values of multi-annual data on three parameters (i.e., air temperature, relative humidity and sunshine hours) of the study area in this study (Table 1).

2.2.3 Cross-section selection

The minimum value of the water level is 45 m according to the observed data. In order to ensure the stability of the model, the minimum water depth is required to maintain more than 5 m. Thus we used the measured cross-section data with the lowest elevation less than 40 m and discarded those data higher than 40 m. Therefore, in this study, the measured cross-section data were only used at the site of 18.4 km away from the dam. We actually simulated the river segment from reservoir dam to backwater area with the length of 22.0 km. We used the cross-section data from the site of 18.4 km away from the dam to represent the segment cross-section from 18.4 km to 22.0 km.

Table 1 Monthly average values of multi-annual data for meteorological factors in Wuxikou Resevoir

Month	Air temperature (℃)	Relative humidity (%)	Sunshine hour (h)
Jan.	7.5	74.0	4.4
Feb.	5.3	77.8	4.5
Mar.	7.3	77.9	3.6
Apr.	11.3	79.8	3.8
May	17.3	79.2	4.2
June	22.1	79.2	5.6
July	25.4	81.1	5.7
Aug.	28.9	76.8	8.5
Sept.	28.5	76.1	9.3
Oct.	24.5	75.9	7.6
Nov.	19.1	74.2	5.8
Dec.	12.9	75.2	4.9

2.2.4 Water temperature

Only Dufengkeng hydrological station, located in the lower reach of the Changhe River and 41 km away from the dam, has long-term series of observed water-temperature data. We collected the observed data from 1964 to 2007 at this station. After the Changhe River and the Le′an River are merged into one river, it is called the Raohe River. Meanwhile, both the Changhe River and the Le′an River have similar geographical position and climate characteristics. Moreover, both Xiangtun and Hushan hydrological stations located in the Le′an River have observed water-temperature data. The Hushan station has the data from 1964 to 2007, while the data from 1964 to 1986 for the Xiangtun station. Both stations are approximately 46 km far away from each other. Therefore, we replaced the raised rate of water-temperature of the Changhe River with that of the Le′an River. We calculated the water temperature of the Wuxikou Reservoir tail and dam based on the monthly average values of multi-annual data at the Dufengkou station. The water temperature data are shown in Table 2.

2.2.5 Water level and discharge flow

The water level and discharge flow data are the necessary boundary condition for the development of hydrological-model. We collected water level and discharge flow data in the early, middle and late of each month in typical year (Table 3).

2.2.6 Mesh calculation

The calculated grid cell size is 1000 m in the mainstream direction of river. There are ten layers of grids

Table 2 Multi-annual average water temperature at Wuxikou Reservoir tail and dam

Month	Temperature rise rate along distance (℃/100km)	Water temperature at dam (℃)	Water temperature at tail (℃)
Jan.	1.2	8.0	7.8
Feb.	0.7	9.4	9.3
Mar.	0.5	12.8	12.8
Apr.	0.5	17.7	17.7
May	0.8	22.0	21.9
June	1.1	25.1	24.9
Jul.	1.6	28.3	28.0
Aug.	2.1	29.2	28.8
Sept.	1.5	26.3	26.5
Oct.	2.3	20.8	20.4
Nov.	2.2	14.9	14.5
Dec.	2.0	9.8	9.4

Table 3 Water level of reservoir and discharge flow in early, middle and late of each month in typical year

Month	Discharge flow			Water level of reservoir		
	Early	Middle	Late	Early	Middle	Late
Jan.	25.6	25.6	25.6	46.6	45.8	45.0
Feb.	50.0	265.6	25.6	53.0	56.0	45.0
Mar.	25.6	25.6	22.9	47.1	46.0	45.8
Apr.	25.6	69.0	160.4	45.0	45.5	50.0
May	365.4	80.3	89.8	50.0	50.0	50.0
June	93.1	233.3	25.6	50.0	50.0	50.0
July	185.3	39.1	49.5	55.8	56.0	56.0
Aug.	29.4	25.6	32.6	56.0	56.0	55.9
Sept.	25.6	25.6	25.6	56.0	55.8	55.6
Oct.	25.6	25.6	25.6	55.0	54.3	53.5
Nov.	25.6	25.6	25.6	52.9	52.2	51.4
Dec.	25.6	25.6	25.6	50.3	48.8	47.4

along water depth direction. The height of the vertical grid varies with the changes in water levels, and the grid cell size can be automatically adjusted. There are approximately 220 meshes in total for the study area.

2.3 Data processing

Thermal equilibrium parameters were used to carry out sensitivity analysis. These parameters included light attenuation, constant in Beer′s law, radiation parameter *A*, radiation parameter *B* and evaporation-first parameter. The first four parameters can impact the solar-radiation absorption of water body, and the last one can affect the evaporation of water body. In order to analyze the parameter sensitivity, the above parameters were given different values to calculate the water temperature in front of the dam and the discharged water temperature. The effect of each parameter value on model results was analyzed to obtain the parameter sensitivity. Finally, key parameters could be screened and identified for the hydrological model. According to the actual situation, the local roughness value (n) is 0.054. Analysis of variance (ANOVA) was performed to identify the differences between simulated water temperature for given values of each thermal equilibrium parameter, between upper and deeper water temperature and between different months. Difference was considered to be significant if $p < 0.05$. Figures for the simulated data were performed using Excel 2010 software package.

3 Sensitivity Analysis of Thermal Equilibrium Parameters

3.1 Light attenuation parameter

The parameter of light attenuation means the solar-radiation attenuation coefficient in the water. The allocation of absorbed solar radiation in each water layer can be expressed by using Beer′s law formula:

$$E_{fac} = I_0(1 - \beta)\exp(-\alpha(D\text{-}z)) \quad (1)$$

where E_{fac} is the light intensity at depth (D-z) below the surface; α is the solar-radiation attenuation coefficient in the water (light attenuation); β is the surface absorption rate (Beer′s law coefficient), and β value is less than 1; I_0 is the light intensity just below the water surface; (D-z) is the distance from water surface to different layer. In order to analyze the sensitivity of light attenuation parameter, the water temperature in front of the dam and the discharged outflow-water temperature were calculated for six different parameter values ($\alpha_1 = 0.3$, $\alpha_2 = 0.65$, $\alpha_3 = 2$, $\alpha_4 = 5$, $\alpha_5 = 10$ and $\alpha_6 = 15$). The water temperature distribution in front of the dam under six different conditions was illustrated to show the prediction results in this study.

Figure 2 shows the vertical distribution of water temperature in front of the dam in January, May, August and November, respectively. During the period from January to February, no stratification could be observed for the deeper water, and the deeper water temperature was slightly lower than the surface water temperature. The

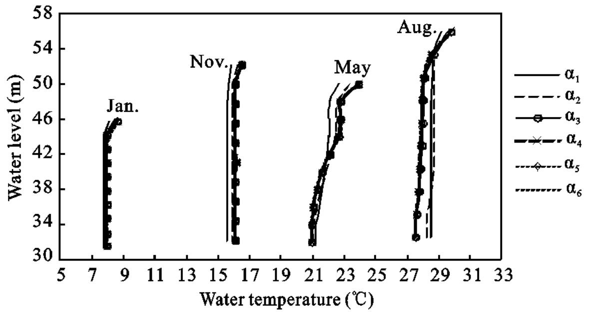

Fig. 2 Vertical distribution of water temperature in front of dam for different α values in different months

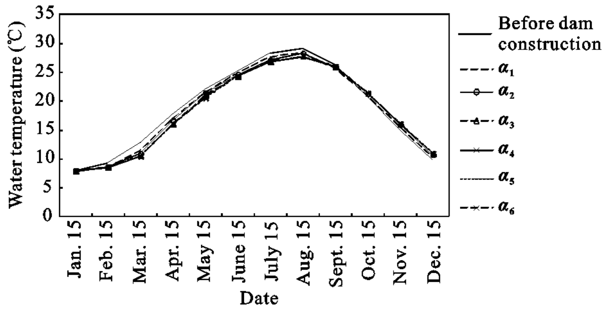

Fig. 3 Monthly changes in discharged outflow-water temperature before and after dam construction

differences of several parameter values for water temperature were not significant ($p > 0.05$). The fitting curves for different parameter values were nearly overlapped except for little difference among surface water temperature with the maximum temperature difference of 0.5℃.

From March to July, water temperature increased gradually, and the upper water temperature did not show much higher values than the deeper one ($p > 0.05$). Water temperature stratification began to occur. However, it was not obvious. The fitting curves had similar changing tendency with no significant difference among them with the maximum temperature difference of 1.3℃ ($p > 0.05$). Additionally, the fitting curves for the parameter values equal to or more than 2 were nearly overlapped.

Water temperature reached the maximum value in August. Similarly, the stratification of water temperature could not be observed for deeper water, and their water temperature was lower than surface water temperature ($p < 0.05$). However, the fitting curves were nearly overlapped for the parameter values equal to or more than 2.

From September to December, water temperature decreased gradually, and the changing tendency of water temperature was similar for each parameter value, indicating higher water temperature for higher parameter values. However, no significant difference was observed among the fitting curves for these given parameter values ($p > 0.05$), with the maximum temperature difference of 0.7℃. Similarly, the fitting curves were nearly overlapped for the parameter values equal to or more than 2.

As shown in Fig. 3, different parameter values did not affect the changing tendency of the discharged outflow-water temperature. During the period from January to September, the water temperature was relatively lower after dam construction than before, while they showed relatively higher values after the dam construction from October to December. Generally, the effects of different parameter values were similar with the maximum temperature difference of 0.4℃. If the given parameter value was equal to or more than 2, the parameter would not impact water temperature and their fitting curves (α_3–α_6) were nearly overlapped. Therefore, the parameter values influencing water temperature ranged from 0.5 to 0.7.

3.2 Constant in Beer's law of solar absorption

In the Beer's law formula, β (Constant in Beer's law) represents solar absorption, and this parameter generally ranges from 0 to 1. The water temperature in front of the dam and the discharged outflow-water temperature in each month of the dry year were respectively simulated for the given seven conditions ($\beta_1 = 0.2$, $\beta_2 = 0.4$, $\beta_3 = 0.5$, $\beta_4 = 0.7$, $\beta_5 = 0.9$, $\beta_6 = 1.0$, and $\beta_7 = 1.5$) in order to analyze the sensitivity of this parameter.

Figure 4 shows the vertical distribution of simulated water temperature in front of the dam in January, March, July and October, respectively. As shown in Fig. 4, if $\beta > 1.0$, the fitting curves demonstrated great difference from those for $\beta \leq 1.0$. Especially from March to August, the difference was very significant ($p < 0.05$). So the simulation results were obviously unreasonable. When β was equal or less than 1.0, the fitting curves for different parameter values were similar during the period from January to February. From September to December, no stratification was observed in deeper water. Especially in January and February, the fitting curves for deeper water temperature were nearly overlapped. Surface water temperature was relatively higher than deeper water temperature ($p > 0.05$). Moreover, the temperature difference between surface water and deeper water increased slightly with increasing β values from March to April, a large increment could be observed in surface water temperature compared to deeper water temperature, but the water temperature stratification was faint with the maximum temperature difference of 3℃. The simulated water temperature for different β values showed an increasing tendency from May to August. However, it was not obvious for water temperature stratification during this period as the maximum temperature difference between the surface and deeper water was about 2℃.

Figure 5 shows monthly changes in the discharged outflow-water temperature for different β values. Except for a larger deviation of the fitting curve for $\beta > 1.0$, other β values had similar effects on the vertical distribution of the discharged outflow-water temperature. During the period from January to September, the discharged outflow-water temperature were relatively lower after the dam construction than before, whereas they had relatively higher values after the dam construction than before from October to December. When β was equal to or less than 1.0, similar effects of β values were observed on the discharged outflow-water temperature ($p > 0.05$). Therefore, the sensitivity of β values was low and ranged from 0.2 to 0.7.

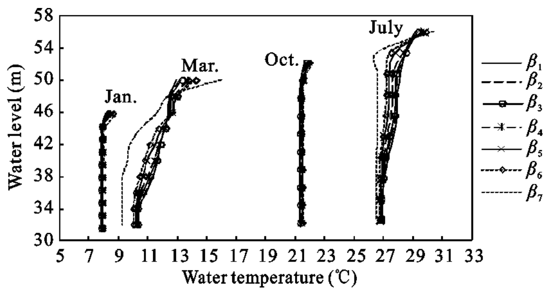

Fig. 4 Vertical distribution of water temperature in front of dam for different β values in different months

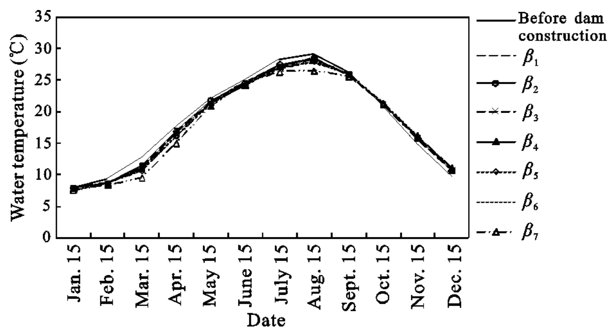

Fig. 5 Monthly changes in discharged outflow-water temperature before and after dam construction

3.3 Radiation parameter *A*

Daily solar radiation can be calculated by the following formula:

$$H/H_0 = A + B(n/N_d) \quad (2)$$

$$A = 0.1 + 0.24(\bar{n} / \bar{N}_d) \quad (3)$$

$$B = 0.38 + 0.08(\bar{N}_d / \bar{n}) \quad (4)$$

where H is the daily radiation under cloudy skies; H_0 is the extraterrestrial intensity in short wave radiation on the surface; n is the amount of sunshine hours; N_d is the length of the day; $\bar{n}$ is the mean annual value of n; $\bar{N}_d$ is the mean annual value of N_d; A and B are adjustable parameters in the model. Parameter A ranges from 0.10 to 0.34 and parameter B is more than 0.48. We analyzed the sensitivity of parameters A and B, respectively.

The water temperature in front of the dam and the discharged outflow-water temperature in each month of dry year were simulated for different given A values ($A_1 = 0.10$, $A_2 = 0.20$, $A_3 = 0.30$, and $A_4 = 0.34$) to identify the sensitivity of parameter A.

Figure 6 demonstrates the vertical distribution of water temperature in front of the dam in January, April, June, and October, respectively. From January to December, the simulated water temperature increased with the increase in parameter A value. It was because that the elevated A value increased solar radiation absorbed by the water body.

Deeper water temperature did not show obvious stratification. The maximum water-temperature difference among different A values was 2.2℃ in January.

Water temperature increased gradually from March to April, the obvious increment in water temperature of upper water could be observed compared to deeper wa-

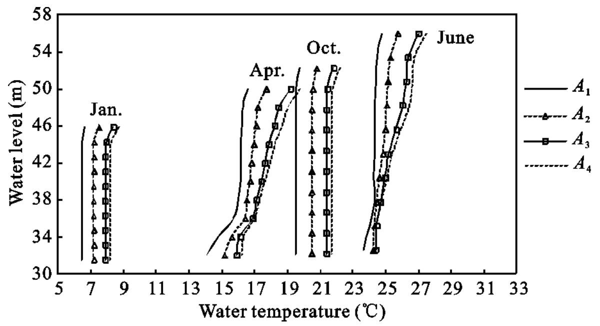

Fig. 6 Vertical distribution of water temperature in front of dam for different A values in different months

ter. The maximum temperature difference between upper and deeper water was 3.0℃. The maximum temperature difference among simulated water temperature for different A values was 3.7℃.

From May to July, water temperature increased continuously, and the changing tendency of water temperature was consistent. However, no obvious water temperature stratification was found. There was a great difference between surface water temperature for different given A values compared to deeper water temperature, and the maximum temperature difference among surface water temperature was 2.6℃.

Similarly, surface water temperature was a little higher than deeper water temperature without obvious stratification from August to December ($p > 0.05$). The simulated water temperature increased with increasing A values, and the maximum temperature difference for different A values was 2.9℃.

Among all months, the maximum of water-temperature difference between $A_2 = 0.20$ and $A_3 = 0.30$ was approximately 1.0℃.

As shown in Fig. 7, the monthly changes in the discharged outflow-water temperature before and after the dam construction are compared. The effects of the parameter A were obvious. When $A_1 = 0.10$, a large deviation could be observed for the fitting curve compared to the other A values. Thus the model result was not reasonable. However, when $A_4 = 0.34$, the fitting curve of the discharged outflow-water temperature was more consistent with the actual case.

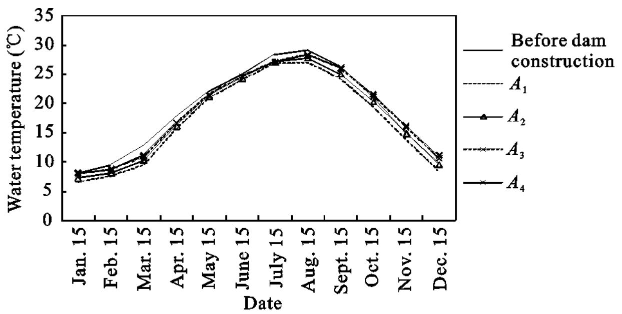

Fig. 7 Monthly changes in discharged outflow-water temperature before and after dam construction

Therefore, parameter A had strong sensitivity and ranged from 0.10 to 0.34, and the model results showed obvious difference among different A values for each month. This parameter should be paid much more attention to numerical simulation.

3.4 Radiation parameter *B*

Water temperature in front of the dam and the discharged outflow-water temperature were simulated for each month of the dry year for different parameter B ($B_1 = 0.40$, $B_2 = 0.48$, and $B_3 = 0.50$) to identify the sensitivity of the parameter B.

Vertical distribution of water temperature in front of the dam for different B values in January, June, and October are shown in Fig. 8. The values of the different B parameters had little effect on the simulation results of the model. Water temperature showed a slight increase with increasing B values. Compared to surface water temperature, the simulated deeper water temperature for different B values were similar. The changing tendency was consistent for three B values. However, when B was less than 0.48, a deviation became obvious.

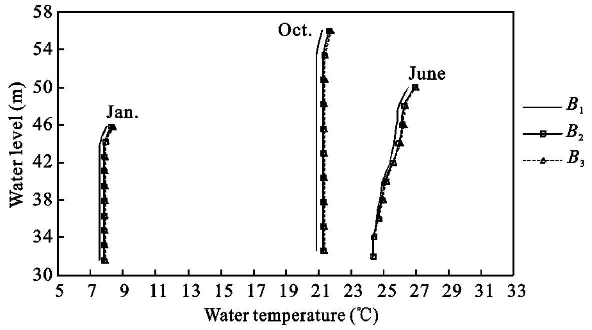

Fig. 8 Vertical distribution of water temperature in front of dam for different B values in different months

In January and February, surface water temperature showed a slight increase compared to deeper water temperature without obvious stratification. No significant difference was found among the fitting curves for different B values ($p > 0.05$), with the maximum temperature difference of 0.38℃. From March to July, water temperature increased gradually with increasing months. Although no obvious stratification was observed, the water temperature rise rate was slightly higher in surface water than that in deeper water ($p > 0.05$). The changing tendency was consistent for different B values, and great difference in surface water temperature among different B values could be observed compared to deeper water temperature, with the maximum temperature difference of 0.57℃. In August, water temperature increased up to the maximum value. Water temperature with no stratification decreased from September to December. The fitting curves for different B

values had similar changing tendency with the maximum temperature difference of 0.60℃.

As shown in Fig. 9, the different B values had little influence on monthly changes in the discharged outflow-water temperature. The sensitivity of the parameter B was not strong. The changing tendency of the discharged outflow-water temperature was consistent and three fitting curves were nearly overlapped from January to September. Generally, these B values were equal to or more than 0.48, while B was less than 0.48, a high deviation would be observed.

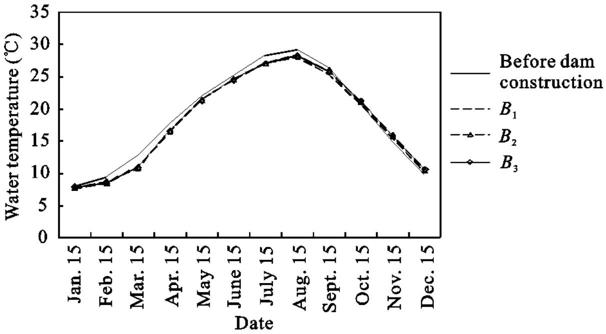

Fig. 9 Monthly changes in discharged outflow-water temperature before and after dam construction

3.5 Evaporation-first parameter

In MIKE 11 model, evaporation is calculated by Dolton formula:

$$q_v = LC_e\ (a + bW_{2m})(Q_{water} - Q_{air}) \tag{5}$$

where q_v is evaporation; L is the latent heat of vaporization; C_e is the coefficient of humidity; W_{2m} is wind speed at 2 m site; Q_{water} is the water-vapor density above water body; Q_{air} is the water-vapor density in the air. For the model, parameters (a and b) need to be calibrated. In this study, wind speed was not taken into account, so the sensitivity of this parameter (b) was not analyzed.

The water temperature in front of the dam and the discharged outflow-water temperature were simulated in each month of the dry year for different values ($a_1 = 1$, $a_2 = 4$, $a_3 = 6$, $a_4 = 8$, $a_5 = 10$, and $a_6 = 15$) to analyze the sensitivity of parameter a.

Vertical distribution of water temperature in front of the dam for different a values in January, July, and November are shown in Fig. 10. During the period from January to December, the fitting curve for $a_1 = 1$ showed great difference from other fitting curves (a_2–a_6). Additionally, there was a significant difference between the fitting curve for $a_2 = 4$ and other fitting curves for $a > 4$

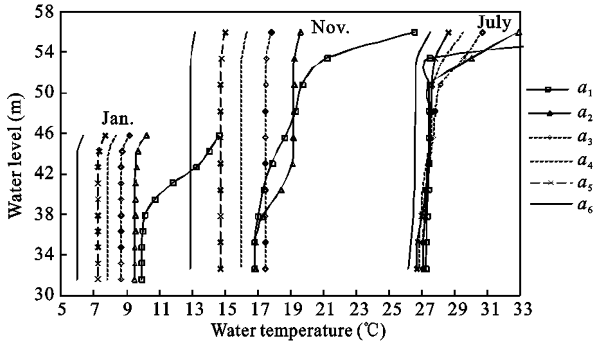

Fig. 10 Vertical distribution of water temperature in front of dam for different a values in different months

(a_3–a_6) from March to December ($p < 0.05$). The four fitting curves for a_3–a_6 demonstrated similar changing tendency of water temperature in all the simulated months, and water temperature decreased with increasing parameter a values.

According to the simulated results, no stratification occurred for water temperature during the periods from January to February and from July to December. Meanwhile, the simulated water temperature for $a > 4$ from July to December (the maximum water temperature difference was 4.7℃) were higher than those from January to February (the maximum water temperature difference was 3.0℃) ($p < 0.05$). Indistinctive stratification was observed during the period from March to June, showing higher water temperature in surface water than deeper water. However, the fitting curves for $a > 4$ showed consistent changing tendency with the maximum water temperature difference of 3.5℃.

As shown in Fig. 11, evaporation-first parameter had great effect on the discharged outflow-water temperature. When $a_6 = 15$, the fitting curve was not reasonable. If $a \leq 10$, the changing trendy of fitting curves was consistent.

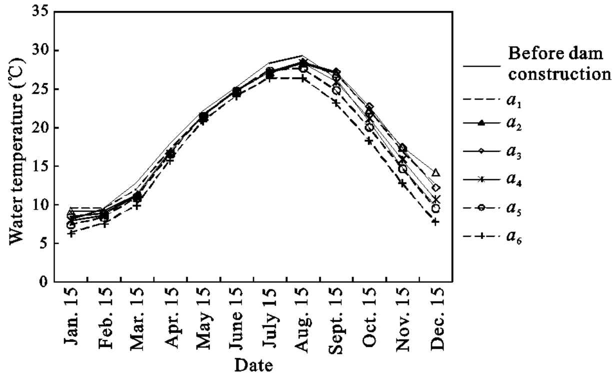

Fig. 11 Monthly changes in discharged outflow-water temperature before and after dam construction

Evaporation-first parameter values had higher sensitivity to surface water temperature, because this parameter could greatly impact evaporation. Therefore, we should throw light on this parameter when the model was calibrated. This parameter generally ranged from 0 to 10. When $a_6 = 15$, the discharged outflow-water temperature was significantly lower after dam construction than before ($p < 0.05$), indicating the model result was not satisfactory. The maximum temperature difference for surface water was 18℃ among the simulated data for different *a* values, and the minimum temperature difference for deeper water was 0℃.

4 Conclusions

In this study, we analyze the sensitivity of these parameters including light attenuation parameter, constant in Beer′s law, radiation parameters *A* and *B*, and evaporation-first parameter. We find that evaporation-first parameter and radiation parameter show higher sensitivity to water temperature among all the above parameters. Thus both parameters were key drivers for model results. According to the simulated data, the reasonable range for these parameters is also identified. Within the scope of reasonable range, variations in parameter values do not significantly impact the discharged outflow-water temperature. Therefore, if we have no observed data to calibrate the model we can input the local empirical values to MIKE 11 model to simulate quantitatively the changes in the discharged outflow-water temperature. It is noted that all thermal equilibrium parameters have little impact on deeper water temperature. The effects of wind are not taken into consideration due to shortage of wind speed and wind direction data in this study. Further studies are still needed to analyze the sensitivity of evaporation parameter *b* to identify the effects of this parameter on model results.

References

Bai J H, Cui B S, Chen B *et al.*, 2011. Spatial distribution and ecological risk assessment of heavy metals in surface sediments from a typical plateau lake wetland, China. *Ecological Modelling*, 222(2): 301–306. doi: 10.1016/j.ecolmodel.2009.12

Bai J H, Gao H F, Xiao R *et al.*, 2012a. A review of Soil nitrogen mineralization in coastal wetlands: Issues and methods. *Clean-Soil*, *Air*, *Water*, 40(10): 1099–1105. doi: 10.1002/clen.201200055

Bai J H, Xiao R, Zhang K J *et al.*, 2012b. Arsenic and heavy metal pollution in wetland soils from tidal freshwater and salt marshes before and after the flow-sediment regulation regime in the Yellow River Delta, China. *Journal of Hydrology*, 450–451: 244–253. doi: 10.1016/j.jhydrol.2012.05.006

Beven K J, Freer J, 2001. Equifinality, data assimilation and uncertainty estimation in mechanistic modeling of complex environ-mental systems using the GLUE methodology. *Journal of Hydrology*, 249(1–4): 11–29. doi: 10.1016/S0022-1694(01)00421-8

Beven K, Binley A, 1992. Future of distributed models: Model calibration and uncertainty prediction. *Hydrological Processes*, 6(3): 279–298. doi: 10.1002/hyp.3360060305

Borgonovo E, Tarantola S, 2012. Advances in sensitivity analysis. *Reliability Engineering & System Safety*, 107: 1–2. doi: 10.1016/j.ress.2012.09.001

Chen Jiongfeng, Zhang Wanchang, 2006. Application of genetic algorithm for model parameter calibration in daily rainfall-runoff simulations with the Xin'anjiang model. *Journal of China Hydrology*, 26(4): 32–38. (in Chinese)

Fan S F, Feng M Q, Liu Z, 2009. Simulation of water temperature distribution in Fenhe Reservoir. *Water Science and Engineering*, 2(2): 32–42.

Hapuarachchi H A, Li Zhijia, Wang Shouhui, 2001. Application of SCE-UA method on parameter optimization of Xin'anjiang model. *Journal of Lake Sciences*, 13(4): 305–314. (in Chinese)

Huang Guoru, Xie Hehai, 2007. Uncertainty analyses of watershed hydrological model based on GLUE method. *Journal of South China University of Technology*: *Natural Science Edition*, 35(3): 137–142, 149. (in Chinese)

Jiang Chunbo, Zhang Qinghai, Gao Zhongxin, 2000. A 2-D unsteady flow model for predicting temperature and pollutant distribution in vertical cross section of a river. *Journal of Hydraulic Engineering*, 31(9): 20–24. (in Chinese)

Lamboni M, Monod H, Makowski D, 2011. Multivariate sensitivity analysis to measure global contribution of input factors in dynamic models. *Reliability Engineering & System Safety*, 96(4): 450–459. doi: 10.1016/j.ress.2010.12.002

Pekárová P, Miklánek P, Halmová D *et al.*, 2011. Long-term trend and multi-annual variability of water temperature in the pristine Bela River basin (Slovakia). *Journal of Hydrology*, 400: 333–340. doi: 10.1016/j.jhydrol.2011.01.048

Wang Guan, Han Longxi, Chang Wenting, 2009. Modeling water temperature distribution in reservoirs with 2D laterally averaged flow-temperature coupled model. *Water Resources Protection*, 25(2): 59–63. (in Chinese)

Wang Q G, Bai J H, Huang L B *et al.*, 2011a. Soil nutrient distribution in two typical paddy terrace wetlands along an elevation gradient during the fallow period. *Journal of Mountain Science*, 8(3): 476–483. doi: 10.1007/s11629-011-1122-y

Wang Q G, Zhao X H, Yang M S *et al.*, 2011b. Water quality model establishment for middle and lower reaches of Hanshui River, China. *Chinese Geographical Science*, 21(6): 646–655. doi: 10.1007/s11769-011-0504-y

Xiao R, Bai J H, Gao H F *et al.*, 2012. Spatial distribution of phosphorous in marsh soils from a typical land/inland water ectone along a hydrological gradient. *Catena*, 98: 96–103. doi: 10.1016/j.catena.2012.06.008

Xiao R, Bai J H, Zhang H G *et al.*, 2011. Changes of P, Ca, Al and Fe contents in fringe marshes along a pedogenicchrono sequence in the Pearl River estuary, South China. *Continental Shelf Research*, 31(6): 739–747. doi: 10.1016/j.csr.2011.01.013

Zak S K, Beven K J, 1999. Equifinality, sensitivity and predictive uncertainty in the estimation of critical loads. *Science of Total Environment*, 236(1–3): 191–214. doi: 10.1016/S0048-9697(99)00282-X

Zhang Jing, Ross M A, Geurink J, 2012. Discretization approach in integrated hydrologic model for surface and groundwater interaction. *Chinese Geographical Science*, 22(6): 659–672. doi: 10.1007/s11769-012-0566-5

Zhang Liru, Guan Yiqing, Ye Bin *et al.*, 2008. Empirical study on parameter sensitivity analysis of Xin'anjiang model. *Water Resources and Power*, 26(5): 16–30. (in Chinese)

Zhang Shi, Peng Wenqi, 2009. Water temperature structure and influencing factors in Ertan Reservoir. *Journal of Hydraulic Engineering*, 40(10): 1254–1258. (in Chinese)